Stellar Mass & Supermassive Black Holes: the Collimated Outflow Phase

Ruth A Daly

Outflows from stellar mass & supermassive black holes can significantly affect their gaseous and stellar environments; for example, X-ray binaries with outflows exist in globular clusters (e.g. Bahramian et al. 2014)

=> working on new methods to estimate/measure BH spin values, accretion disk magnetic field strengths, mass accretion rates, & radiant efficiency factors, + …

⇒ new method, the "Outflow Method," proposed & developed by D16, D+18, D19, & D21 (+ D09a,b; D11).
=> outflows carry magnetic fields that are generated and maintained in accretion disks, which may be important in regulating star formation (e.g. Daly & Loeb 1990; Fall 2000; …)

Locally, about half of all AGN have jet powered outflows, and of the 756 AGN that will be discussed today, only about 100 are considered to be "radio loud," though all of the sources have jetted outflows.
Thus, this may be a standard phase that AGN cycle through (e.g. Nagar, Falcke, Wilson, Ulvestad 2002)

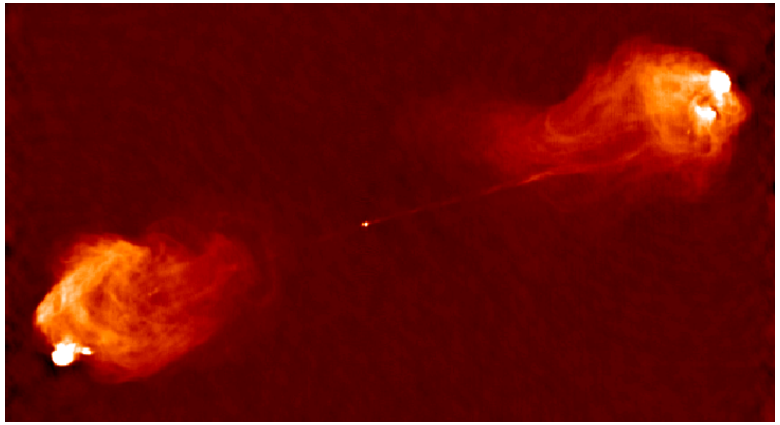

1) Review the empirical motivation of the outflow method
2) describe its application and review some current results

Four samples of very different types of sources were selected for study:
102 measurements of 4 stellar mass BH (XRB); 100 FRII sources; 576 LINERS; 80 Local AGN

Key empirically determined ingredients:

L_j = outflow beam power, dE/dt (in kinetic energy), (strong shock method & the fundamental line mapping method)
L_{bol} = accretion disk bolometric luminosity, (from [OIII] and (2-10) keV luminosities)
L_{Edd} = black hole mass (i.e. Eddington luminosity), (Obtained with standard, well-accepted techniques)

These quantities are combined to obtain BH spin, accretion disk magnetic field strength, + other properties such as mass accretion rates and efficiency factors.

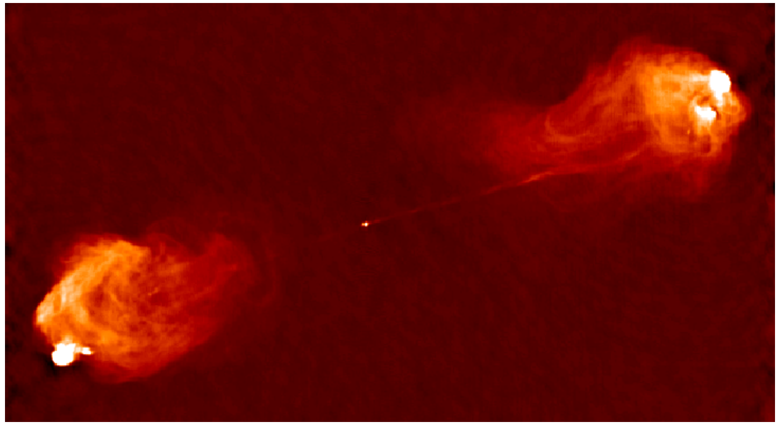

BH Systems with Disk and Outflow Activity (D+18)
=> All governed by the same physical processes

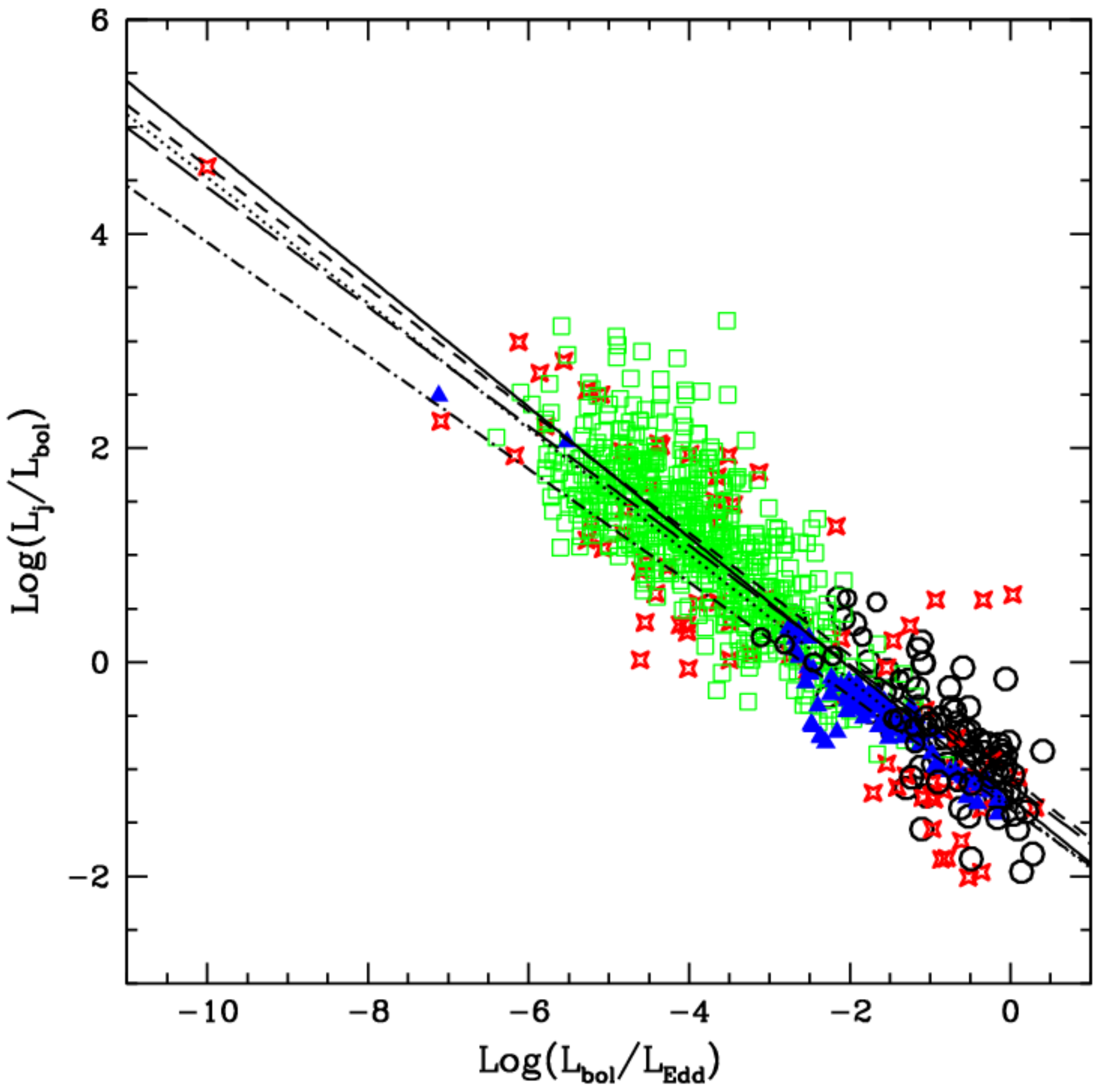

4 Categories of BH considered (D+18):

3 types of supermassive BH +
1 type of stellar-mass BH

100 FRII sources - shown in black (D16)
576 LINERs (Nisbet & Best 2016) – shown in green
80 AGN (Merloni et al. 2003) – shown in red
102 (of 4) Stellar-mass XRB (Galactic black holes) – shown in blue (Saikia et al. 2015)

Best fit slopes (A-1):
-0.56 ± 0.05 for 100 FRII sources (long-dashed line)
-0.57 ± 0.02 for 576 LINERs (med-dashed line)
-0.59 ± 0.04 for 80 Compact RS AGN (dotted line)
-0.53 ± 0.02 for 102 GBH (dot-dashed line)
The solid line shows the fit to all sources (from D+18)

$(L_j/L_{bol}) \propto (L_{bol}/L_{EDD})^{A-1}$ **Strictly empirical**

(No accretion disk or outflow model is assumed; suggests spin powered outflow)

BH Systems with Disk and Outflow Activity (D+18)
=> All governed by the same physical processes

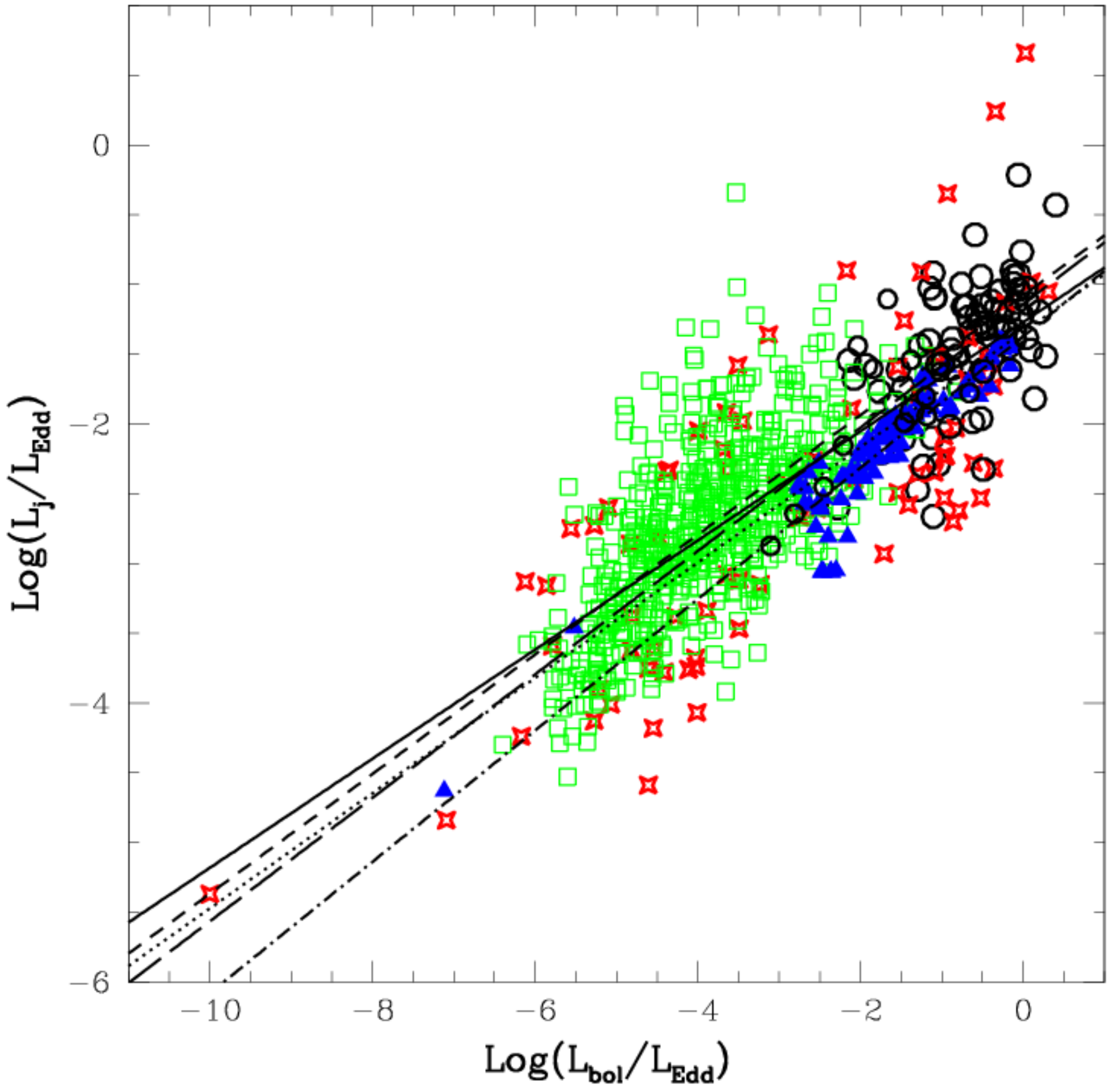

4 Categories of BH considered (D+18):

3 types of supermassive BH +
1 type of stellar-mass BH

97 FRII sources - shown in black (D16)
576 LINERs (Nisbet & Best 2016) – shown in green
80 AGN (Merloni et al. 2003) – shown in red
102 Stellar-mass Galactic black holes – shown in blue (Saikia et al. 2015)

Best fit slopes A:

0.44 ± 0.05 for 97 FRII sources (long-dashed line)
0.43 ± 0.02 for 576 LINERs (med-dashed line)
0.41 ± 0.04 for 80 Compact RS AGN (dotted line)
0.47 ± 0.02 for 102 GBH (dot-dashed line)
The solid line shows the fit to all sources (from D+18)

=> $(L_j/L_{Edd}) \propto (L_{bol}/L_{EDD})^A$ Strictly empirical

(No accretion disk or outflow model is assumed)

Empirically studies of L_j , L_{bol} , L_{EDD} indicate:

$$(L_j/L_{Edd}) \propto (L_{bol}/L_{EDD})^A$$ (empirical relationship D16, D+18)

Theoretical expectation for spin powered outflow models (e.g. Blandford & Znajek 1977; Meier 1999), is **$L_j \propto B_p^2 L_{Edd}^2 F^2$**. This can be re-written in dimensionless-separable-form (DSF):

$$(L_j/L_{Edd}) = g_j (B/B_{Edd})^2 F^2$$ Theoretical Eq. for spin powered outflow model in DSF (D19)

B = disk field strength; $(B_p/B)^2$ is absorbed into g_j; & $B^2_{Edd} \propto M^{-1} \propto (L_{EDD})^{-1}$ (e.g. Rees 1984)

B_p => poloidal component of B field - anchored in accretion disk and threading the BH region

=> $$(B/B_{Edd})^2 = (L_{bol}/L_{EDD})^A$$ (D19, D21) Can be derived with other methods

$\Rightarrow$ $$B = B_{Edd} (L_{bol}/L_{EDD})^{A/2}$$ since $B^2_{Edd} \propto M^{-1} \propto (L_{EDD})^{-1}$ (e.g. Rees 1984)

=> $$F^2 = f(j)/f_{max} = (L_j/g_j L_{Edd}) (L_{bol}/g_b L_{Edd})^{-A}$$ (D16,D19) Can be derived with other methods

where $F = (f(j)/f_{max})^{1/2} = j/[1+ (1 - j^2)^{1/2}]$ **[requires $j \leq 1$, so empirical values of $F > 1$ => $j = 1$]**

j => dimensionless black hole spin, sometimes denoted a_* or a in other work

With L_j and L_{bol} normalized by L_j (max) = g_j L_{EDD} and L_{bol} (max) = g_b L_{EDD}

Results shown indicate $g_j = 0.1$ and $g_b = 1$; take these throughout (see empirical results of D+18)

576 LINERS (NB16) 80 Local AGN (M03) 100 FRII AGN (D16/D19) 102 measurements of 4 GBH (S15)

$\delta \mathrm{Log}(B/B_{Edd}) \approx 0.10, 0.12, 0.13$, and 0.06 & $\delta \mathrm{Log}(B_4) \approx 0.22, 0.23, 0.37$, and 0.06 for LINERs, FRIIs, M03, GBH

$(B/B_{Edd}) = (L_{bol}/L_{Edd})^{A/2}$ varies by AGN type

$B = (B/B_{Edd})\,(6/M_8^{1/2}) \times 10^4$ G

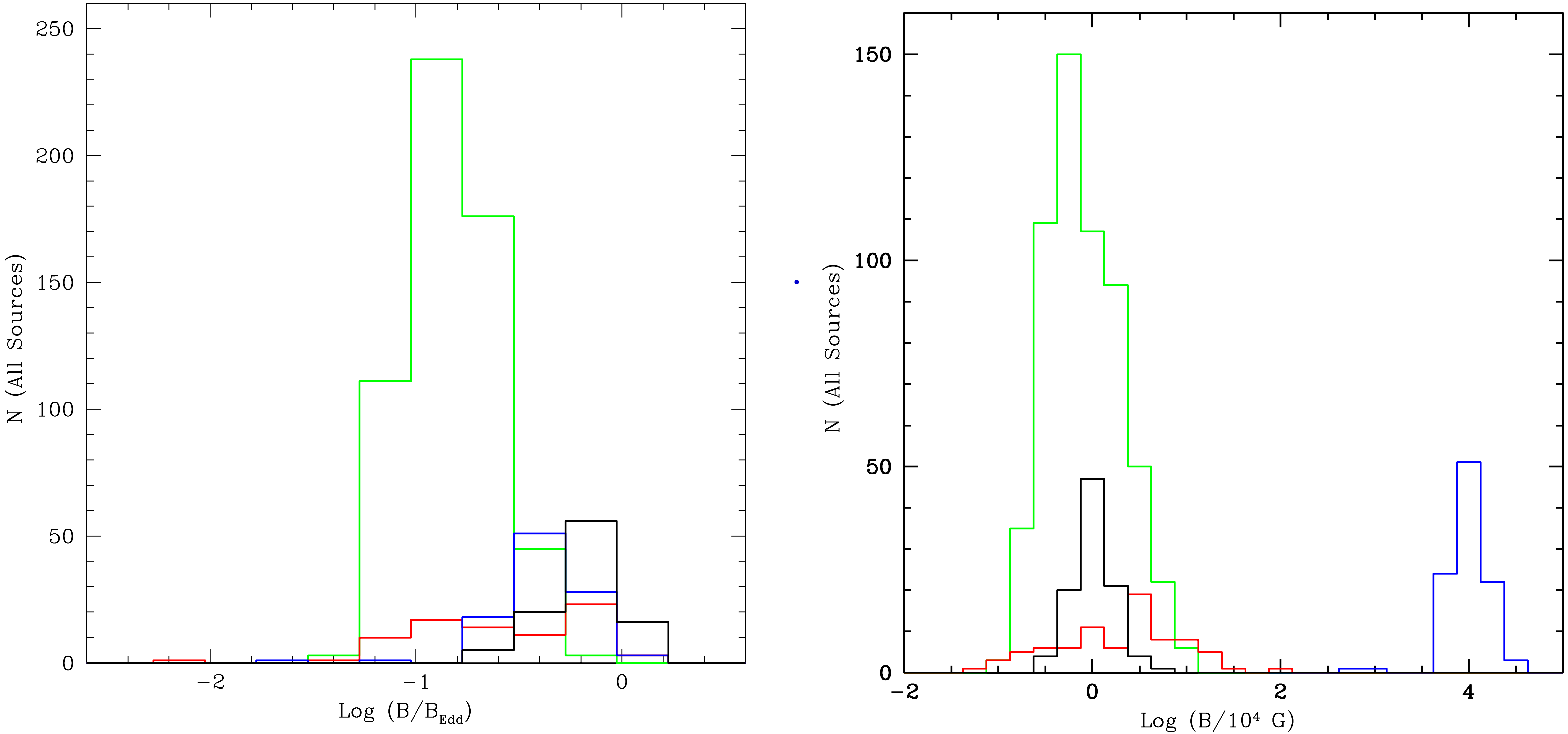

576 LINERS (NB16)   80 Local AGN (M03)   100 FRII AGN (D16/D19)   102 measurements of 4 GBH (S15)

B_4 = $(B/B_{Edd})\ (6/M_8^{1/2})$ $\delta Log(B_4) \approx$ 0.22, 0.23, 0.37, and 0.06 for LINERs, FRIIs, M03, GBH

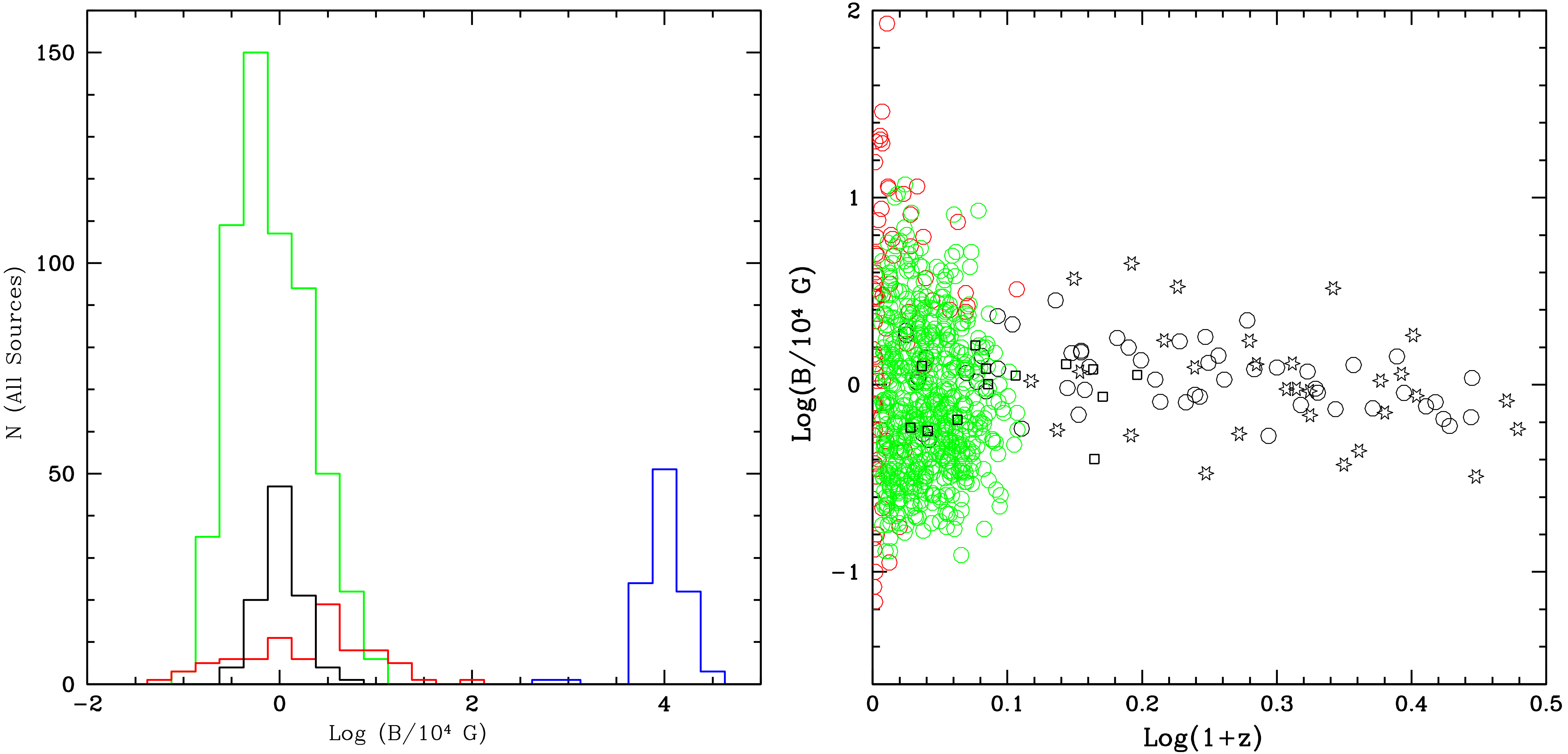

LINERs
FRII RS
Compact RS
X-R-Binaries

Table 1. Mean Value and Standard Deviation of Histograms and Values for Select Individual Sources. [a]

(1) Sample	(2) Type	(3) N [b]	(4) $\mathrm{Log}\sqrt{(f(j)/f_{max})}$	(5) j	(6) j_{pub} (ref)[c]	(7) Log(B/B$_{Edd}$)	(8) Log(B/10^{4}G)
NB16(1)[d]	AGN	576	$-0.04 \pm 0.24(0.14)$	0.93 ± 0.10		$-0.83 \pm 0.21(0.10)$	$-0.09 \pm 0.39(0.22)$
D16	AGN	97	$-0.07 \pm 0.19(0.15)$	0.93 ± 0.11		$-0.19 \pm 0.17(0.12)$	$0.03 \pm 0.23(0.23)$
M03	AGN	80	$-0.17 \pm 0.36(0.19)$	0.81 ± 0.20		$-0.58 \pm 0.42(0.13)$	$0.27 \pm 0.66(0.37)$
S15	GBH	102	$-0.17 \pm 0.10(0.07)$	0.92 ± 0.09		$-0.37 \pm 0.23(0.06)$	$4.00 \pm 0.24(0.06)$
GX 339-4	GBH	76	-0.17 ± 0.06	0.92 ± 0.06	0.94 ± 0.02 (1)	-0.32 ± 0.18	4.07 ± 0.18
GX 339-4					$0.95^{+0.03}_{-0.05}$ (2)		
V404 Cyg	GBH	20	-0.10 ± 0.06	0.97 ± 0.02		-0.44 ± 0.24	3.84 ± 0.24
XTE J1118 [e]	GBH	5	-0.43 ± 0.01	0.66 ± 0.02		-0.54 ± 0.01	3.80 ± 0.01
AO6200 [f]	GBH	1	-0.08 ± 0.07	0.98 ± 0.07		-1.62 ± 0.06	2.76 ± 0.06
Sgr A^*	AGN	1	-0.17 ± 0.19	0.93 ± 0.15		-2.09 ± 0.13	-0.61 ± 0.37
M87 [g]	AGN	1	0.13 ± 0.19	1.00 ± 0.15		-1.19 ± 0.13	-1.16 ± 0.37
Ark 564	AGN	1	0.06 ± 0.19	1.00 ± 0.15	$0.96^{+0.01}_{-0.11}$ (3)	0.17 ± 0.13	1.93 ± 0.37
Mrk 335	AGN	1	-0.29 ± 0.19	0.81 ± 0.15	> 0.91 (3)	-0.15 ± 0.13	1.06 ± 0.37
Mrk 335					$0.70^{+0.12}_{-0.01}$ (4)		
Mrk 335					$0.83^{+0.10}_{-0.13}$ (5)		
NGC 1365	AGN	1	0.53 ± 0.19	1.00 ± 0.15	> 0.84 (3)	-0.64 ± 0.13	0.70 ± 0.37
NGC 4051	AGN	1	-0.02 ± 0.19	1.00 ± 0.15	> 0.99 (3)	-0.34 ± 0.13	1.30 ± 0.37
NGC 4151	AGN	1	-0.27 ± 0.19	0.84 ± 0.15	> 0.9 (3)	-0.35 ± 0.13	0.60 ± 0.37
3C 120	AGN	1	0.59 ± 0.19	1.00 ± 0.15	> 0.95 (3)	-0.13 ± 0.13	0.78 ± 0.37

[a]Obtained for $g_{bol} = 1$ and $g_j = 0.1$ for all sources. The estimated uncertainty per source is included in brackets following the standard deviation in columns (4), (7), and (8) for the samples listed in the top part of the table, as discussed in section 3.3. The bottom part of the table includes entries for three individual GBH, which have multiple observations per source, one additional GBH, and several individual AGN.

[b]N is the number of sources for the AGN and the number of measurements for the GBH.

[c]Published spin values; the citations are: (1) Miller et al. (2009); (2) Garcia et al. 2015; (3) Vasudevan et al. (2016); (4) Patrick et al. (2012); and (5) Walton et al. (2013).

To study mass accretion rates (dM/dt) and (dm/dt) and efficiency factors (D21):

$L_j \propto (dM/dt)\, F^2$ => $(L_j/ L_{Edd}) = g_j\, (dm/dt)\, F^2$ where $(dm/dt) = (dM/dt)\, c^2/L_{Edd}$

Compare with new dimensionless separable representation of equation describing a spin powered outflow [D19]: **$(L_j /L_{Edd}) = g_j\, (B/B_{Edd})^2\, F^2$**

=> $(dm/dt) = (B/B_{Edd})^2 = (L_{bol}/L_{EDD})^A$ and **$(dM/dt) = (L_{bol}/L_{EDD})^A\, L_{Edd}\, c^{-2}$**

In addition, **$L_{bol} = \varepsilon_{bol}\, (dM/dt)\, c^2$ => $\varepsilon_{bol} = (L_{bol}/L_{Edd})\, (B/B_{Edd})^{-2} = (L_{bol}/L_{EDD})^{1-A}$**

Thus $\varepsilon_{bol} = (L_{bol}/L_{EDD})^{1-A} = (dm/dt)^{(1-A)/A} \approx (dm/dt)^{1.2}$ for $A \approx 0.45$

No specific accretion disk model is assumed

Also define $\varepsilon_{s/d} = F^2/(dm/dt)$ => provides measure of spin/accretion contribution to (L_j/L_{Edd})

It turns out that $\varepsilon_{s/d} = g_j^{-1}\, (L_j/L_{bol})\, (L_{bol}/L_{Edd})^{1-2A} \approx g_j^{-1}\, (L_j/L_{bol})\, (L_{bol}/L_{Edd})^{0.1}$ for $A \approx 0.45$

Table 2. Comparison of Accretion Rates and Bolometric Efficiency Factors Obtained Here with Independently Determined Values (see section 4).

(1) Source	(2) Type	(3) J19 (dm/dt)	(4) This Work (T5) (dm/dt)	(5) Ratio (T5)/J19
Ark 564	NS1	1.70	2.21	1.30
Mrk 279	S1.5	0.75	0.48	0.64
Mrk 335	NS1	0.74	0.51	0.69
Mrk 590	S1.2	0.31	0.61	1.97
PG 0804 + 761	Q	1.13	0.43	0.38
PG 0844 + 349	Q	1.20	0.42	0.35
PG 1229 + 204	Q	0.50	0.65	1.29
PG 1426 + 015	Q	0.28	0.21	0.75

(1) Source	(2) Type	(3) R12 (T1) (dM/dt) $(M_\odot\ yr^{-1})$	(4) This Work (T5) (dM/dt) $(M_\odot\ yr^{-1})$	(5) Ratio (T5)/R12(T1)	(6) R12 (T3) ϵ_{bol}	(7) This Work (T5) ϵ_{bol}	(8) Ratio (T5)/R12(T3)	(9) R12 (T2) ϵ_{bol}	(10) Ratio (T5)/R12(T2)
Mrk 279	S1.5	0.045	0.045	1.00	0.25	0.35	1.40		
Mrk 509	NS1	0.095	0.082	0.86	0.29	0.37	1.28	0.46	0.80
NGC 5548	S1.5	0.006	0.067	11.64	0.98	0.16	0.16		
NGC 7469	S1	0.083	0.010	0.12	0.21	0.60	2.86	0.26	2.31
3C 120	S1	0.178	0.065	0.37	0.16	0.42	2.63		
3C 390.3	S1	0.062	0.202	3.28	0.36	0.15	0.42		

576 LINERS (NB16) 80 Local AGN (M03) 100 FRII AGN (D19) 102 measurements of 4 GBH (S15)

$\dot{m} = (B/B_{Edd})^2 = (L_{bol}/g_b L_{Edd})^A$ varies by type; $\delta \text{Log}(dm/dt) \approx 0.2, 0.24, 0.26$, and 0.06 for LINERs, FRIIs, M03, GBH

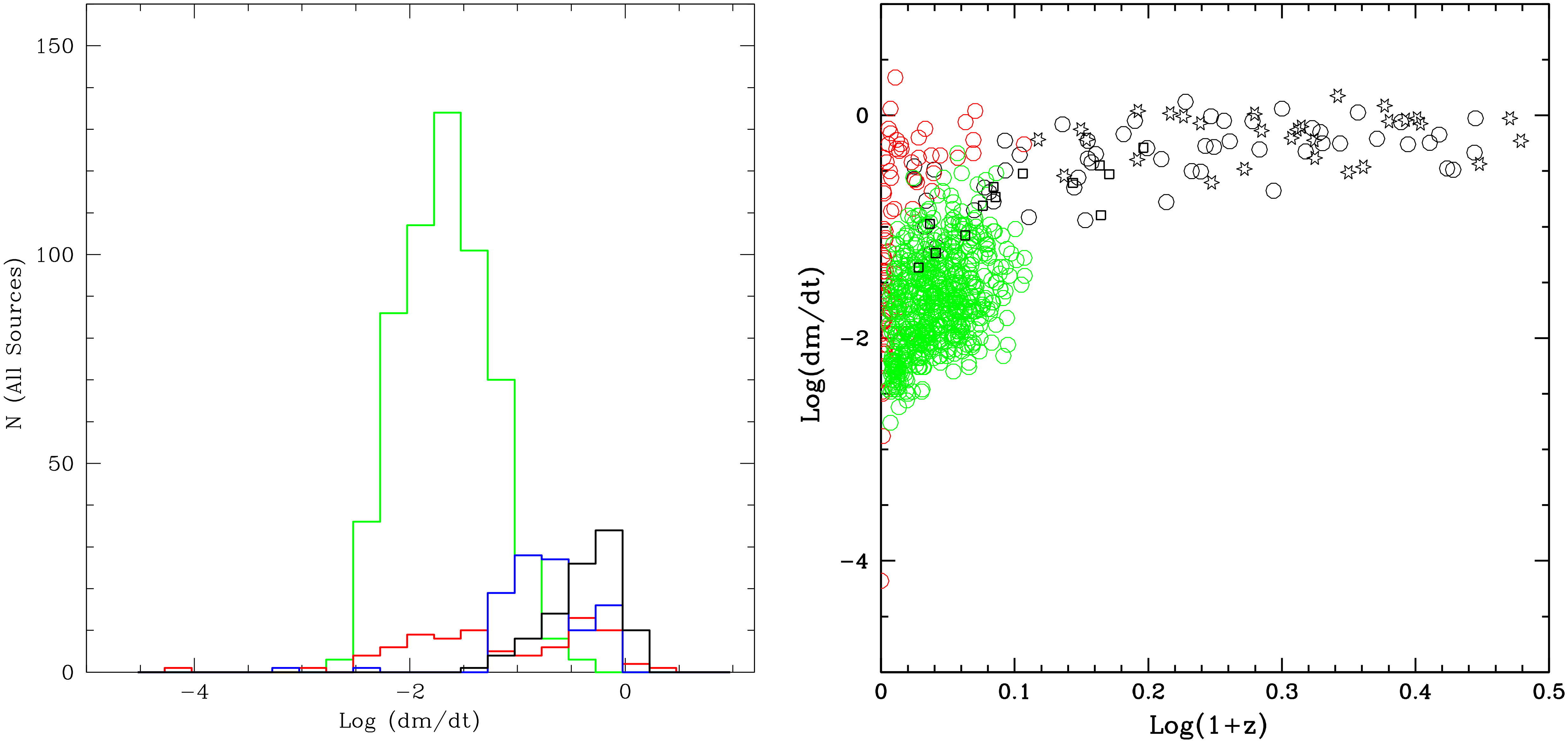

D21 576 LINERS (NB16) 80 Local AGN (M03) 100 FRII AGN (D19) 102 measurements of 4 GBH (S15)

$\dot{M} = \dot{m}\, L_{EDD} / c^2$ or $\dot{M} = (B/B_{edd})^2\, L_{EDD} / c^2$ $\delta \mathrm{Log}(\dot{M}) \approx 0.22, 0.23, 0.37$, and 0.06 for LINERs, FRIIs, M03, GBH

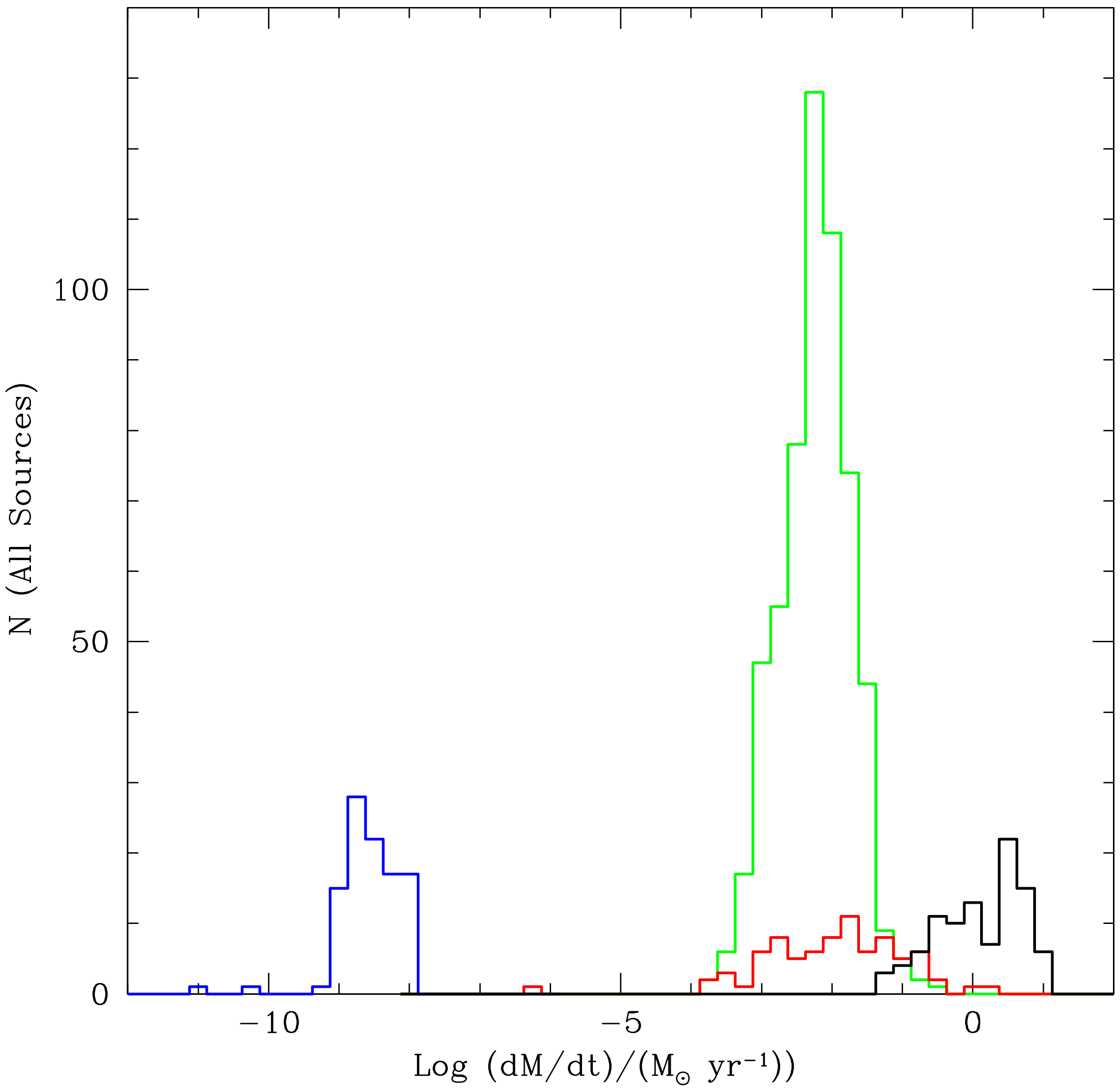

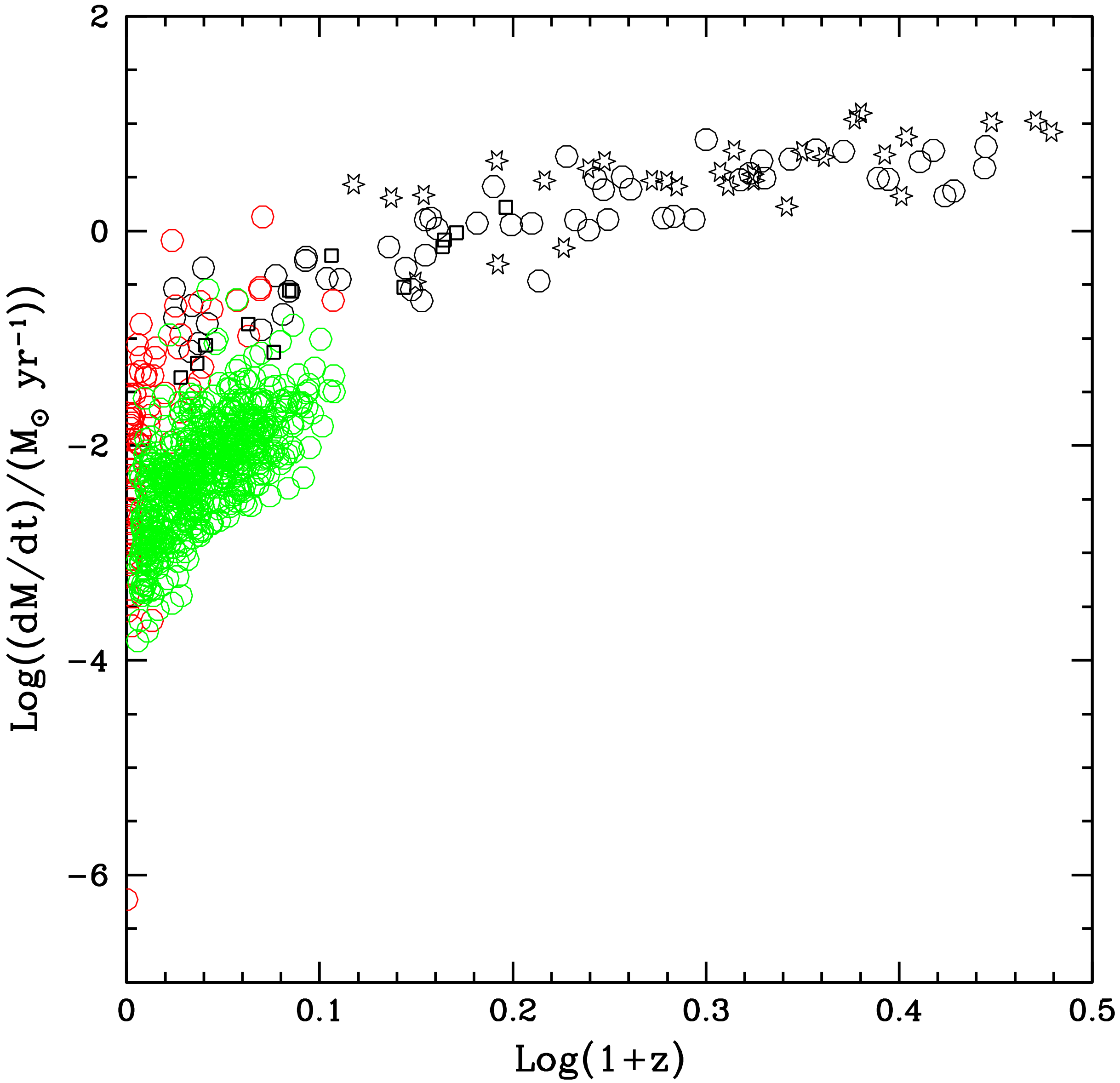

D21 576 LINERS (NB16) 80 Local AGN (M03) 100 FRII AGN (D19) 102 measurements of 4 GBH (S15)

$\varepsilon_{bol} = L_{bol}/(\dot{M}\, c^2) = (L_{bol}/L_{Edd})^{1-A}$ $\delta \mathrm{Log}(\varepsilon_{bol}) \approx 0.24, 0.29, 0.32$, and 0.15 for LINERs, FRIIs, M03, GBH

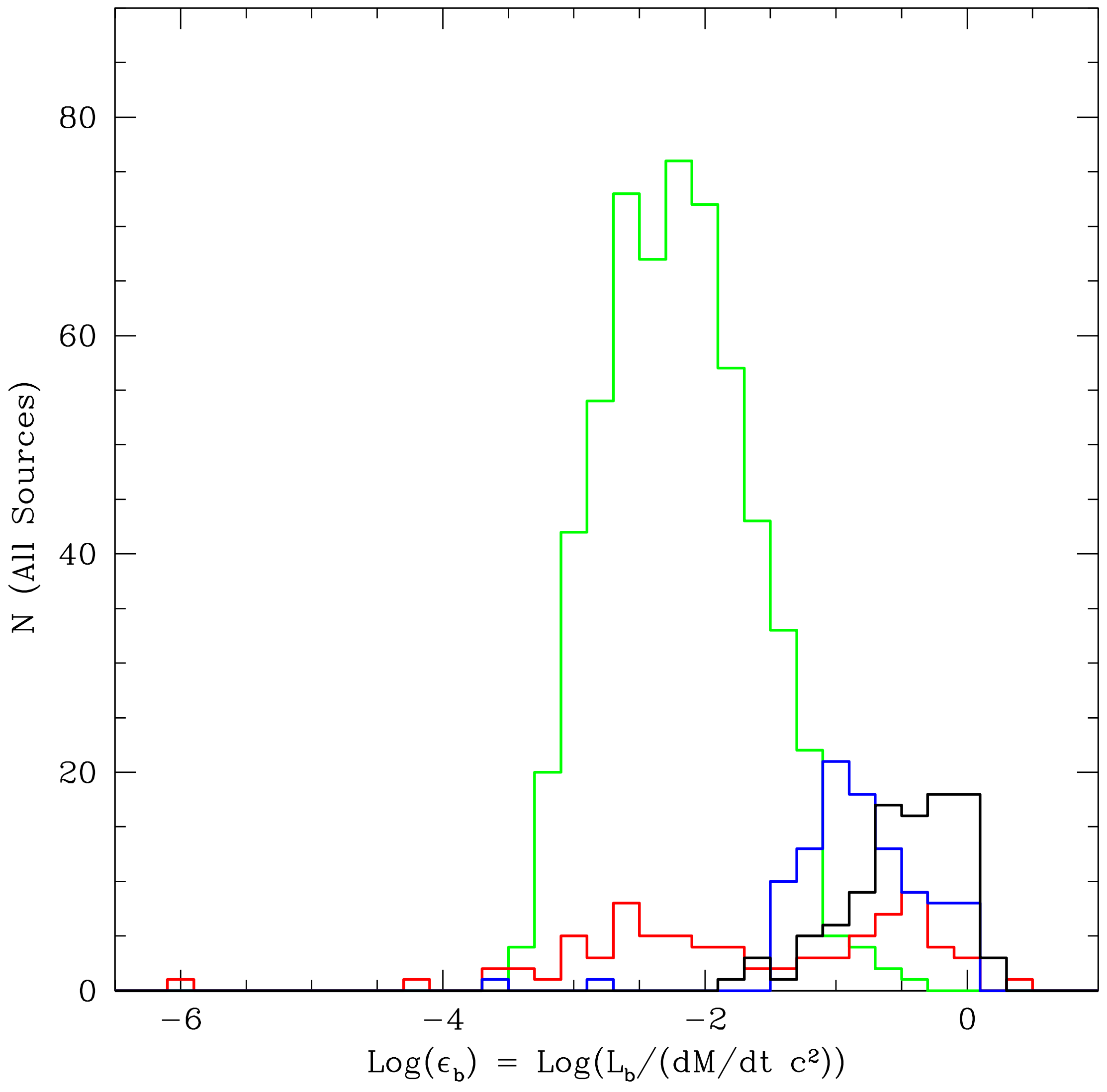

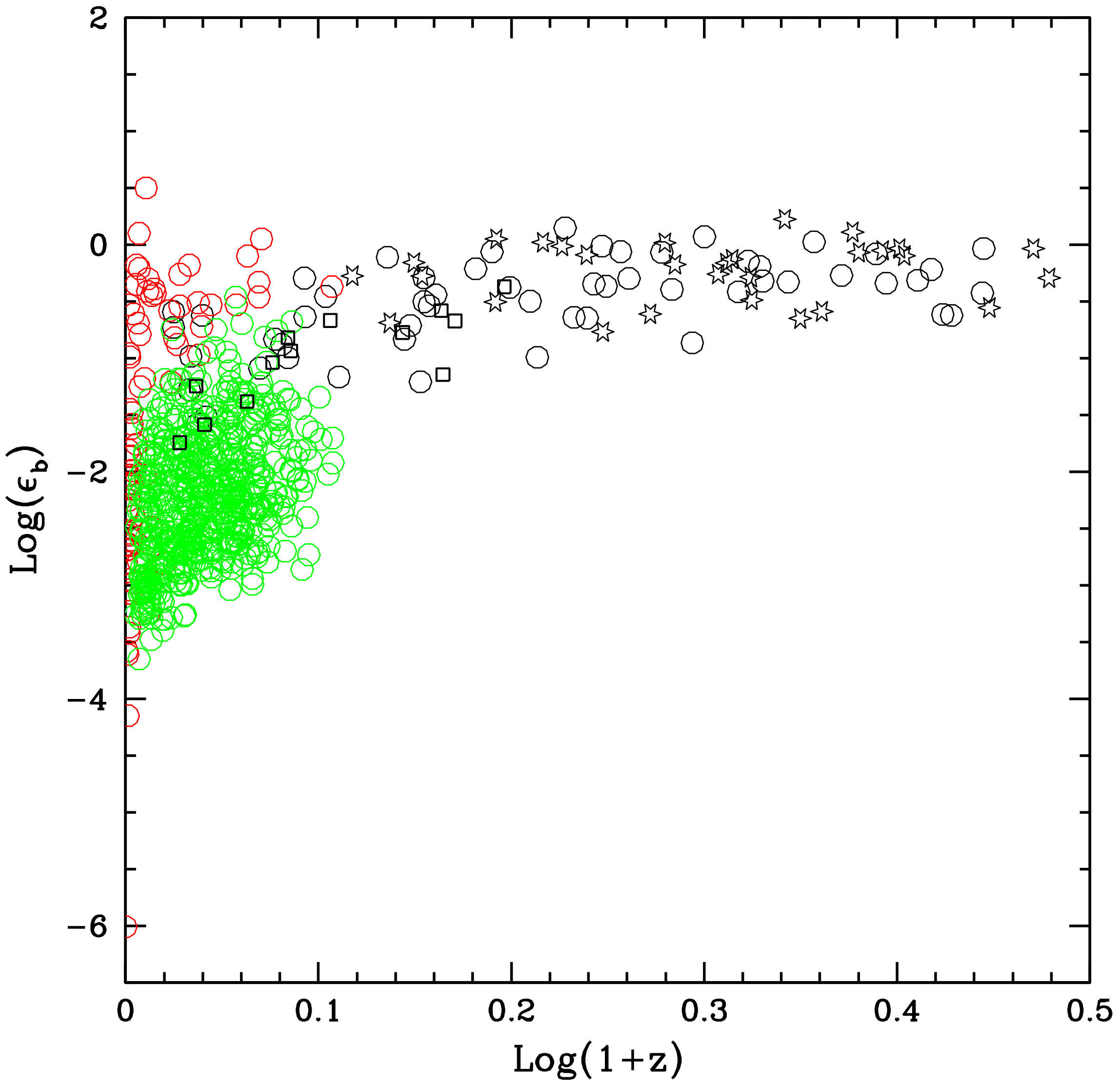

Key Results Obtained to Date with the Outflow Method

I). Outflows from black hole systems inject energy and magnetic fields into their environments, which affects subsequent star formation

II). The Outflow Method allows empirical estimates/determinations of magnetic field strengths, mass accretion rates, black hole spin values, bolometric efficiency factors, and other parameters for these systems.

III). Good agreement between disk B field strengths, mass accretion rates, and bolometric efficiency factors with those obtained independently in the context of specific disk models (and that do not include the existence of outflows)

IV). Good agreement spin values obtained with the outflow method and other methods, such as the X-ray reflection method (Comparison possible for one XRB, GX 339-4, and 6 AGN; Miller et al. (2009); Patrick et al. (2012); Walton et al. (2013); Garcia et al. (2015); & Vasudevan et al. (2016)) **and the continuum fitting method applied to 3CR sources** (Comparison possible for 15 sources, and there is excellent agreement; Azadi et al. 2020)

V). Black hole spin is unrelated to source type for the 4 categories of BH systems studied:
Spins are similar for GBH, LINERS, local AGN (S&L), & classical double (FRII) sources => HEG, LEG, & Quasars

VI). Method and results are empirically based => independent of any specific accretion disk or jet model (in terms of Lorentz factor of outflow, outflow angle, etc.). Thus, the results can be used to study and constrain accretion disk and jet formation models.